Predicting and Detecting Carbonate Cemented Zones Within Latrobe Group Reservoirs of the Gippsland Basin

***Mark Bunch**

Australian School of Petroleum

University of Adelaide, South Australia

mark.bunch@adelaide.edu.au

SUMMARY

A wireline log model predicts carbonate cemented zones within Late Cretaceous to Paleocene reservoir sandstones of the Latrobe Group, Gippsland Basin. Predictions match published evidence. These sandstones were once heavily cemented prior to development of secondary porosity that produced the world-class petroleum reservoirs we see today. Cemented zones that remain must act as obstructions to reservoir fluid migration. They may also react with the mild carbonic acid that will be introduced by CO_2 storage operations of the future. Model predictions show that cemented zones are sparse, spatially sporadic and fall well below seismic resolution at modern-day reservoir depths. Their significance and irregular spatial occurrence mean there is a need to map their distribution.

Synthetic seismograms generated for a number of Gippsland Basin wells predict high amplitude seismic reflectors away from major lithostratigraphic boundaries. Many occur where cemented zones are predicted. An investigation of the complex seismic trace demonstrates seismic sensitivity to these zones in the frequency range 100-125 Hz. An elevated moving average of instantaneous frequency correlates with some of them as does a modified instantaneous Q-factor. Others are indicated by a change in the difference of normalised instantaneous amplitude between the original frequency-filtered complex trace and a frequency-filtered complex trace composed of sinusoids with the same magnitude and phase (arithmetic averages of components of the original complex trace passed after frequency filtering). These subtle phase disturbances at high seismic frequencies are hypothesized to be caused by the presence of thin cemented zones. This idea is tested using instantaneous attributes calculated from 3D seismic survey data available across the Gippsland Basin.

Key words: carbonate cement, Gippsland Basin, wireline log, seismic attributes, Hilbert transform.

INTRODUCTION

A model has been developed to relate the occurrence of zones of carbonate cemented sandstone observed in core sections with a suite of commonly available wireline logs. The model is a 6-attribute fuzzy logic approach (Darling, 2005) that predicts the probability of carbonate cementation using raw (i.e. non-detrended) wireline log data (Bunch, in prep). The model is trained using the Paaratte Formation, a heterolithic siliciclastic deltaic succession deposited from the Santonian through to the Maastrichtian in the Otway Basin (GSV, 1995; Partridge, 2001). It is the final wholly marine unit deposited under a broad sea level regression recorded by the Sherbrook Group supersequence (GSV, 1995). The most viable conventional reservoir units within the Paaratte Formation are compositionally and texturally mature sandstones representing proximal mouthbar deposits. Petrologically these reservoir units are similar to other compositionally and texturally mature conventional siliciclastic reservoirs within shallow marine successions. Latrobe Group sandstone reservoirs of the Gippsland Basin have a similar maturity profile even though their shallow marine depositional environment differs (they are predominantly coastal plain, barrier bar and shoreface marine sandstones; Bishop, 2000; Bernecker and Partridge, 2005).

Carbonate cemented zones occur pervasively within lower reservoir units of the Paaratte Formation. It is thought these zones developed soon after sediment was buried, primarily because petrography shows frequent occurrence of floating matrix grain texture (Daniel et al., 2012). There is spatial association between carbonate cementation and the most texturally and compositionally mature primary sandstone matrix. Presumably, these units were the most permeable sections through which carbon-bearing meteoric groundwater could readily discharged beneath the shallow marine water column. Cementation is thought to have occurred at the interface of fresh and saline waters somewhere within the submarine sediment column (e.g. Taylor and Gawthorpe, 2003).

It is important to understand the distribution of carbonate cementation within conventional siliciclastic reservoir systems. Such cementation may compartmentalise the reservoir system, reducing its bulk permeability and making reservoir sweep a complex process (White et al., 2004). In the case of CO_2 injection (for enhanced oil recovery or as dedicated sequestration operations), their presence would increase reactivity of the reservoir matrix with carbonic acid that develops in formation fluid surrounding free CO_2 (Ott and Oedai, 2015). Dissolution of carbonate cements would later be followed by cement precipitation from what becomes an oversaturated formation fluid. This cycle (which occurs over some spatial extent) would cause usually static fluid flow variables of the reservoir system to become dynamic, perhaps significantly so over the lifespan of operations. Flow system dynamics will therefore always be transient, making it difficult to plan how best to develop the system and optimise fluid flow operations. An understanding of the distribution of carbonate cementation provides the opportunity to incorporate reactivity modelling within flow simulations so future physical states of the reservoir system can be predicted and planned for in advance (e.g. Ott and Oedai, 2015).

The wireline cementation prediction model (CPM) was developed at a single well – the model well (MW) – and was tested both there and at other local wells. The closest of surrounding wells has a well head a mere 173 m away. It was not possible to confidently correlate individual cemented zones between the two wells despite predicted cementation being confirmed in image log data from each well. This gives an indication that such cemented zones can be limited in lateral extent even though the reservoir units/geobodies that host them are expected to extend much further. Cemented zones at the MW were observed to have a mean thickness of ~87 cm (standard deviation of 79 cm), which is well below the limit of seismic resolution (estimated to be ~20 m) at their depth of most frequent occurrence (1400-1500 m). Analogue studies propose an ideal flattened oblate-prolate spheroidal geometry to such cemented zones (Dutton et al., 2000; Dutton et al., 2002); cementation was therefore likely not along a front-like locus but occurred in isolated patches. Arguments for a laterally discrete, pod-like geometry are tenuously supported by statistical evidence at the MW. The proportion of the total thickness of host geobodies (proximal mouthbars) that has been carbonate cemented best follows a Weibull distribution with a shape parameter ('k') greater than 1. In this context, such a distribution implies a cumulative growth process (thicker units get thicker still) rather than one that nucleates then abandons cementation loci permanently. So the spatial distribution of cemented zones and their geometries should be predictable once the relative timing and location of their nucleation centres are known. The sequence stratigraphic architecture that can provide some of this information is below seismic resolution at the MW. Statistical models to make such predictions can be designed using the small pool of data recorded by outcrop analogue studies, e.g. Dutton et al. (2000); Dutton et al. (2002); Taylor and Gawthorpe (2003); White et al. (2004); Lee et al. (2007).

The Gippsland Basin hosts thick, relatively homogeneous conventional siliciclastic reservoirs of younger age that were once heavily cemented by carbonate (Bodard et al., 1984). This paper seeks to demonstrate the distribution of any cementation that remains within these reservoir units directly using customised seismic attributes. The simpler geology of Gippsland reservoirs should mean that subtle seismic signals caused by the presence of distinct but seismically unresolvable acoustic units (such as pods of pervasive carbonate cementation) might not be overwhelmed by interference with higher amplitude reflection events at major lithological boundaries.

METHOD AND RESULTS

The CPM was easily applied to available wireline log datasets at the Gippsland Basin wells featured by Bodard et al. (1984). The model produces two main logs: a probability of cementation log, and a binary 'cemented/not cemented' indicator log that is determined by applying a unique (calculated) probability threshold to the former. Sonic slowness and bulk density wireline logs were used to generate synthetic seismograms for each of these wells. A source wavelet was designed to mimic 3D seismic survey data of the 3D-Geo Gippsland Megavolume (McLean and Blackburn, 2013), though zero-phase was applied to minimise destructive reflection interferences and thereby maximise resolution. A Ricker source with a modal frequency of 30 Hz and a sampling frequency of 4 ms was convolved with the log-derived reflection coefficient series.

Some seismograms show amplitude increases that coincide with predicted cementation zones and some do not. Were these zones seismically resolvable, amplitude increases would be expected because predicted cementation coincides with a marked decrease in P-wave sonic slowness and a marked increase in bulk density. However, they are below seismic resolution so associated seismic reflection event interferences could result in an increase or decrease of seismic amplitude, or any degree of change between.

To maximise the chance of measuring a detectable signal arising from primary seismic reflections at cemented zone boundaries, the resolution of the synthetic seismograms has to be maximised. Such low thickness acoustic units are effectively invisible to the majority of the frequency range of the source wavelet, responding instead to units 10s of metres thick. A high frequency band-pass filter was therefore applied to each synthetic seismogram to isolate the frequency components that would be most sensitive to more closely spaced top and base acoustic boundary reflectors. This was done by calculating a Fast Fourier Transform and reconstructing the seismogram in a forward sense, admitting only the frequency components within the high frequency pass band. The Fast Fourier Transform produced the complex Cartesian components of the frequency-filtered synthetic seismogram comprising the real seismic trace and the Hilbert Transform (Taner et al., 1979; Barnes, 2007). This provided the opportunity to generate a full suite of

commonly derived instantaneous seismic attributes (see: http://doc.opendtect.org/5.0.0/doc/od_userdoc/content/app_a/inst.htm). Significant excursions of attribute curves at around the two-way time range corresponding to the depth for predicted cemented zones, made possible the isolation of a sub-group of instantaneous attributes that may show sensitivity to the presence of cemented zones in real seismic field data. The sensitivity of cemented zone-related attribute curve excursions to the range of the frequency pass band was also explored in order to optimise the range of frequency that would produce the clearest correlation response. Interactive testing produced an optimal frequency pass band of 100-125 Hz for the synthetic seismograms tested.

The shape of a seismogram is conferred by modal frequency components of the amplitude spectrum for the incident wavelet at acoustic impedance boundaries, with distinct sub-seismic resolution acoustic units being effectively filtered from the seismogram by destructive interference between adjacent reflection responses. Components of the pass band produce a conversely filtered seismogram that exhibits strong autocyclicity (acoustic beats at frequency equal to the width of the band, 25 Hz) with little apparent response to the main reflectors seen to generate the full-bandwidth seismogram. This indicates that the amplitude range of the beats oscillation is greater than the net interference amplitude associated with major acoustic impedance boundaries in the frequency range of the pass band. Equivalent beats for the full-band seismogram have a period of 8 ms – at the Nyquist limit – but they are drowned out by modal frequency response, which is a broader set of reflections combining most of the incident wavelet energy and not as susceptible to destructive interference at the spatial scale of the synthetic reflection coefficient series. A larger amplitude, longer period beat signature is seen that corresponds to the frequency difference between successive pass band components. The period depends on the length of the Fourier series but typically for these seismograms is either 1.024 seconds or 2.048 seconds.

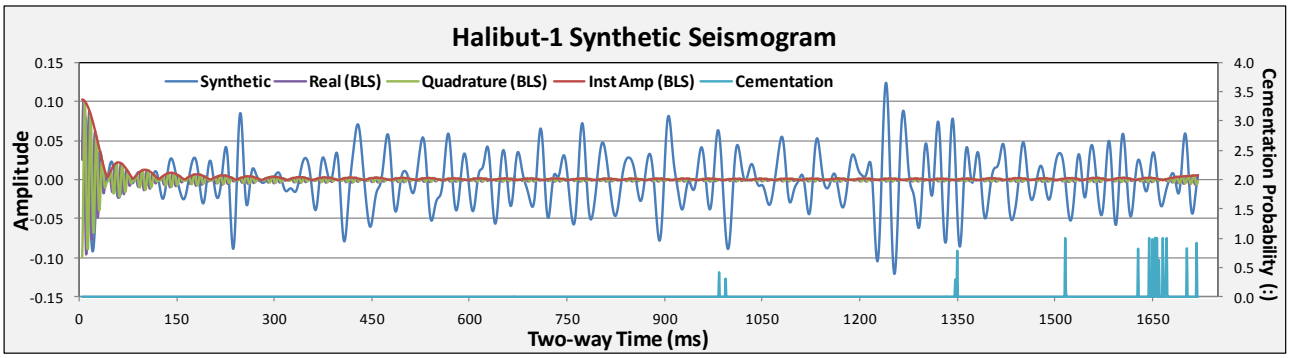

Figure 1: An example of an original synthetic seismogram and the envelope (instantaneous amplitude) over the real and imaginary components of the Band-Limited Seismogram. Note the short and long period beats in band-limited attributes.

Dominance of autocyclic amplitude variations in the band-limited seismograms (BLSs) presents a problem when looking for disturbances caused by particular seismic reflection events. On the presumption that subtle changes to the autocyclic shape of BLSs are encoded in their amplitude and phase spectra, idealised version of BLSs were generated by constructing seismograms adopting the magnitude-weighted arithmetic average of phase, and arithmetic average of magnitude, for each frequency component of the pass band. The idealised BLSs (IBLSs) thereby provided a standard against which increases or decreases in amplitude deviation could be measured at any point along a BLS. Normalising both BLSs and IBLSs (to produce nBLSs and nIBLSs) using a dynamic envelope for peaks and troughs, provided a way to eliminate the effect on amplitude of both the long and short period beats. Stretching and squeezing of the period of oscillation in nBLSs relative to nIBLSs could therefore be measured and taken to represent the net interference effect of small spatial scale reflection events. Given that both nBLSs and nIBLSs are amplitude-normalised, an instantaneous proxy for the stretch and squeeze would be a change in the apparent amplitude difference between the two. For simplicity, this was not converted to an overall phase difference between them so periodic crossover of seismograms and reversal of amplitude difference polarity occurs. This problem was overcome by taking the difference of instantaneous amplitudes for each seismogram, eliminating polarity reversals. A moving median average was used to smooth/remove the periodic dips to zero caused when nBLSs cross. Significant excursions of such an attribute were correlated with predicted cementation for a number of the Gippsland Basin test wells.

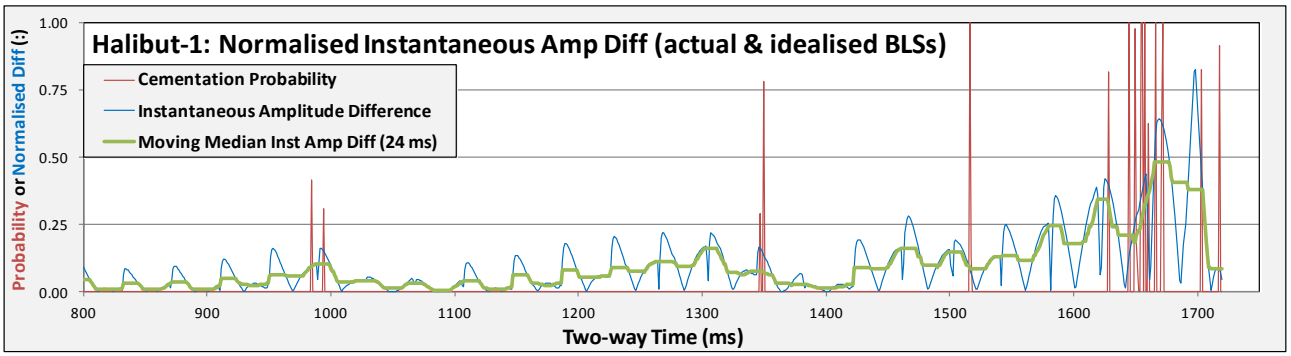

Figure 2: An example of the Normalised Instantaneous Amplitude Difference seismic attribute developed between Band-Limited Seismograms and an 'idealised' version of them generated using the average magnitude and phase for all frequency components.

Two other more basic instantaneous seismic attributes calculated directly from the original BLSs were seen to vary in proximity to most predicted cementation zones. Both are related to instantaneous frequency (phase 'rotation' rate), the first being instantaneous frequency (IF) itself. The short-period beats are evident in the IF attribute. Beat amplitude troughs confer a sudden apparent reversal of complex vector rotation, producing a 'negative' spiked trough in IF that quickly builds again to the average frequency of pass band components. This autocyclic behaviour often become disturbed within or adjacent to cemented zones where IF generally rises a little above the average of frequency components and perhaps even spikes (phase rotation acceleration) at the point when a beats reversal would have occurred. This is an indication that sharper seismogram amplitude gradients have been created by significant constructive interference of spatially proximal reflection events, perhaps close to the tuning frequency.

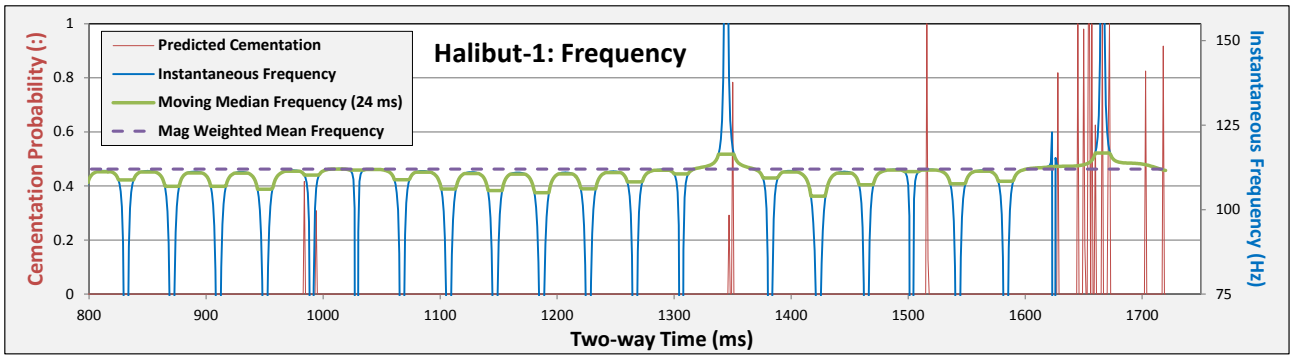

Figure 3: An example of the Instantaneous Frequency seismic attribute developed from Band-Limited Seismograms.

The final instantaneous attribute that appears to respond to the predicted occurrence of cementation is the instantaneous Q-factor. This is the ratio of the instantaneous frequency and the instantaneous bandwidth. The instantaneous bandwidth is the absolute value of the instantaneous amplitude gradient. Beats signatures are again clear for this attribute but orders of magnitude excursions of the median average trend are correlated only with predicted cementation zones. The same explanation would apply for this attribute as was suggested for IF. When excursions do not occur it is possible that any cemented zone/non-cemented zone bundles do not alternate with a wavelength equal to a quarter of the seismic tuning wavelength (on the assumption that they exist at all). Given the relative stability of the instantaneous amplitude attribute with respect to IF, it is obvious that frequency changes are responsible for excursions of this attribute. In order to isolate excursions from the background beats-dominated response, a modified Q-factor attribute was calculated by using the excess of instantaneous frequency above the average of pass band components in the numerator for the calculation (or zero if at or below the average).

Code was written to generate these three instantaneous attributes for entire seismic survey datasets. The 3D-Geo Gippsland Megavolume (McLean and Blackburn, 2013) was processed within the two-way time (TWT) window 568-2612 ms below seismic datum. This range provided 512 sample points per wiggle trace (sampled at 4 ms intervals) thereby facilitating a quick Fast Fourier Transform calculation. The TWT window chosen covers the full converted TWT range for cemented zones predicted at nine offshore Gippsland Basin wells by the CPM. Each attribute volume was subsequently smoothed first per wiggle trace by a 7-sample point centred median filter, then per TWT horizon by a 7-sample (inline/crossline) diameter centred circle. These three smoothed seismic attribute volumes were normalised, then combined in a product to generate a so-called cementation probability volume (CPV). This was then compared at well locations with predictions made by the CPM.

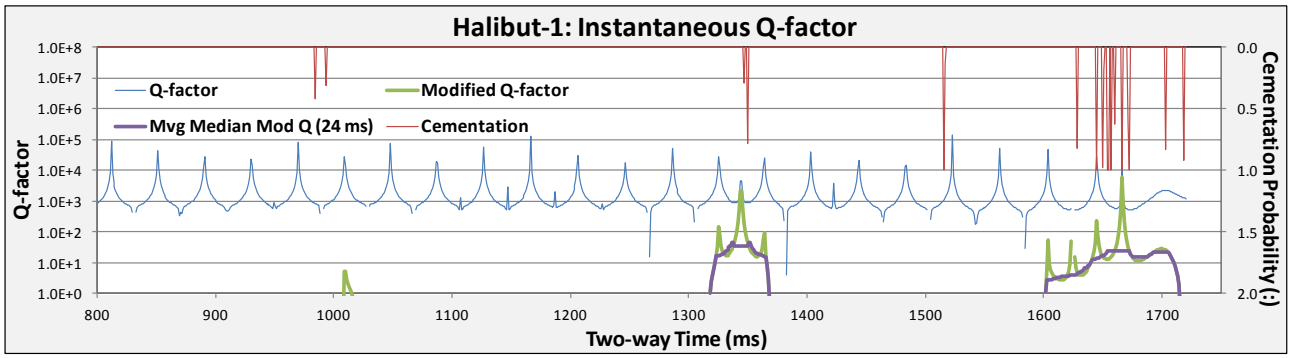

Figure 4: An example of the Modified Instantaneous Q-factor seismic attribute developed from Band-Limited Seismograms.

In general, the distribution of maximum values in the CPV is sporadic and somewhat evenly spread throughout the seismic volume. Most anomalies occur within the siliciclastic Latrobe Group succession but some strong anomalies occur within the cold water carbonates of the overlying Seaspray Group. These units are thought to consolidate markedly with depth, especially within the Albacore Subgroup where cementation and pressure solution are thought responsible for particularly high acoustic velocities (Holdgate et al., 2000; McLean and Blackburn, 2013). Strong CPV anomalies may depict such low porosity zones.

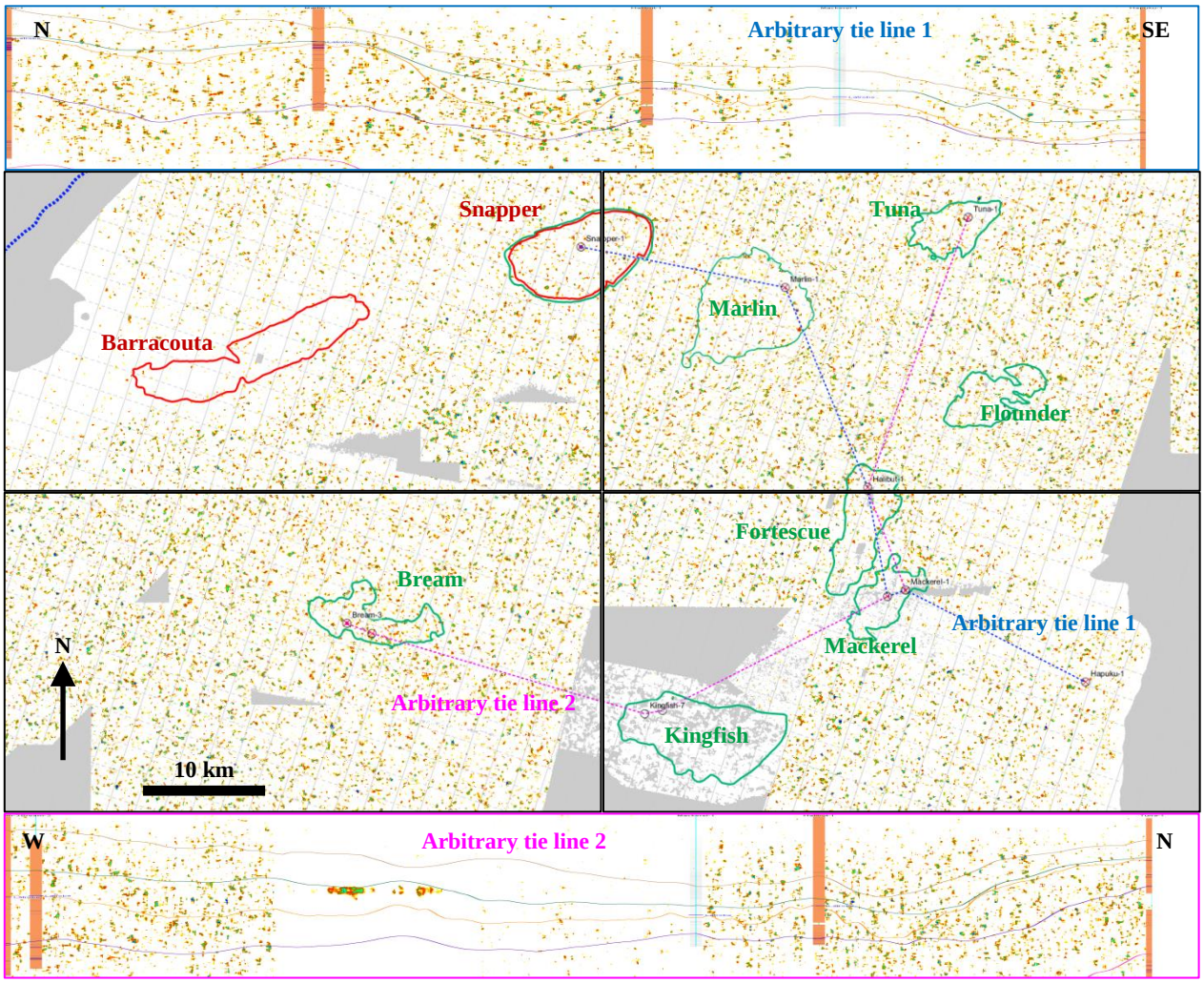

Figure 5: Top & bottom are two arbitrary well ties through the CPV (568-2612 ms). Published horizons (top-bottom) are: mid-Miocene Unconformity (brown), top Lakes Entrance (blue), top Latrobe (orange), K-T boundary (purple). The four central panels show the top Lakes Entrance (top left), top Latrobe (top right), K-T boundary (bottom left) and 50:50 proportional slice between the latter two (bottom right).

The larger anomalies seem concentrated within the central portion of the basin. Their geometry varies from circular in plan-view to more elongate. Some larger structures (~1 km in lateral dimension) appear to have a circular ring-like geometry. When viewed with reduced vertical exaggeration, the geometry of anomalies in 3D can be described as being an oblate spheroid. Most anomalies exhibit a diameter of a few hundred metres or less.

CPV anomalies do not correlate well with cemented sections predicted at wells by the CPM. Some of the highest probability cemented zones are well predicted by CPV anomalies whereas others are not. The best cases of correlation between the CPM and CPV anomalies show a very precise match in their range of depth/TWT. There are some cases where a high CPM excursion appears to correlate with the edge of a CPV anomaly that extends and thickens away from the well. There are also however, cases where a strong CPV anomaly coincides with a low CPM/baseline value.

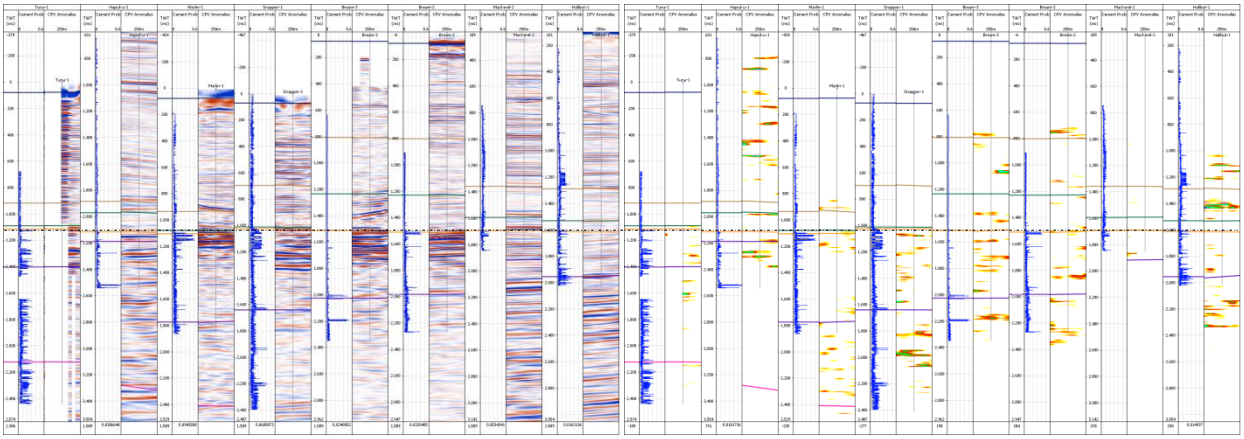

Figure 6: Well panels showing cementation logs (blue) next to surrounding seismic data (125 m either side of the well trace). The left-hand image shows Gippsland Megavolume seismic data. The right-hand image shows CPV anomaly seismic data. Well panels are flattened on the top Latrobe Group well marker (dashed) near-midway up each image. Depth is in TWT.

There are a number of reasons why the CPV would not perform well as a predictive tool for the occurrence of sub-seismic resolution acoustic units. The primary reason is that it cannot be expected to reproduce the response predicted by synthetic seismograms owing to relatively low signal-to-noise ratio (SNR) of the 3D-Geo Gippsland Megavolume seismic data in the range of the frequency pass band. The field data are relatively limited in bandwidth owing to anelastic attenuation of the field source seismic wavelets as they propagated through stratigraphy. This is not simulated in the synthetic seismograms but would act to increase the tuning thickness for alternating cemented/non-cemented zone bundles. This would mean the CPV is sensitive to a different scale of feature than are the synthetic seismograms, even if the acoustic properties of the units comprising such features remain constant. The field survey data also bear overprints of both random and coherent noise; the former will have been suppressed by seismic survey data processing as much as possible but the latter is both a function and possibly also a product of processing. Coherent noise that could not be suppressed or was introduced by processing will have produced artefacts that could create instantaneous attribute anomalies. These arguments are non-specific but may explain cases where a CPM cemented zone does not appear as a CPV anomaly. They are less adequate but still valid in explaining CPV anomalies showing no apparent CPM signature.

The CPM responds not to only to acoustic velocity and bulk density, as the CPV does, but it also responds to neutron porosity, gamma ray, and both shallow and deep resistivities. There is therefore a stronger lithological constraint on this model than can be the case for the CPV. For example, the CPM does not predict a cementation anomaly in the presence of a heterolithic succession of alternating sandstones and shales. Such an arrangement at the right spatial scale could however cause constructive interference of seismic reflection events (with or without a tuning component) that might resemble a compound response generated by a similar arrangement of cemented and non-cemented sandstone units. CPV anomalies are therefore not limited to the subset that might be caused by cementation. 'False positive' CPV anomalies are therefore to be expected. On the other hand, even synthetic instantaneous attributes failed to respond to CPM cementation anomalies in a couple of wells. These cases demonstrate that there is not a firm correlation between the presence of cementation and excursions of the chosen instantaneous attributes. What is not represented explicitly by the CPM probability log is the pervasiveness of cementation. An uneven cementation density might act to 'absorb' the seismic signal by destructive interference of reflection events caused by spatially thin acoustic units. An additional effect relevant to field data is the possibility of acoustic scattering (oblique seismic reflections and refractions) caused by a dipping and/or curved surface geometry of small cemented zones.

The generally even distribution of CPV anomalies through the seismic volume implies that there is no palaeogeographic constraint on their occurrence. The hypothesis for development of the cemented zones within the Paaratte Formation, Otway Basin – cemented

zones that underpin the CPM – is that they formed within (and are therefore constrained by) the geometry of deltaic geobodies. Conventional reservoirs of the Gippsland Basin are shallow marine/shoreface sandstones that extend across the width of the basin parallel to palaeoshoreline barrier bars. Cemented zones within these sandstones might develop sporadically along the paleoshoreface and in that case, would be expected to produce aligned CPV anomalies. There are no obvious correlation trajectories running parallel to the palaeoshoreline for anomalies observed so far within the CPV. Again, given that many anomalies are expected to be caused by features that do not correspond to cemented zones, it may not be possible to identify such trends for those anomalies that do.

CONCLUSIONS

A set of instantaneous seismic attributes was designed using frequency filtered synthetic seismograms to identify zones of carbonate cementation that are below seismic resolution within conventional reservoir sandstones. Not all attributes responded to all predicted cases of cementation at all tested wells. The attributes were calculated for a basin-scale merged 3D seismic survey dataset to produce a combined attribute seismic volume. This volume shows a sporadic distribution of anomalies, some of which correspond strongly to zones of cementation at tested wells but many of which do not. Cemented zones are argued to represent only a subset of stratrigraphic features that might generate combined attribute anomalies. In addition, field seismic data inherently have a lower signal-to-noise ratio than synthetic seismograms. Anomaly signals associated with the stratigraphic features of interest - patches of cementation within sandstones - may therefore not emerge sufficiently from background noise to be easily identifiable.

ACKNOWLEDGMENTS

This work required use of the following specialist software: Petrel Seismic-To-Simulation software by Schlumberger; OpendTect seismic interpretation software by dGB Beheer BV; DUG Insight seismic interpretation software by DownUnder GeoSolutions.

REFERENCES

Barnes, A.E., 2007. A Tutorial on Complex Seismic Trace Analysis. Geophysics, **72**(6), pp. W33–W43.

Bishop, M., 2000. Petroleum System of the Gippsland Basin, Australia. U.S. Geological Survey Open-File Report **99-50-Q**, 36 pp.

Bodard, J.M., Wall, V.J. and Cas, R.A.F., 1984. Diagenesis And The Evolution Of Gippsland Basin Reservoirs. The APPEA Journal, **24**(1), pp. 314-335.

Daniel, R., Menacherry, S. and Bunch, M., 2012. Characterisation of Dolomitic Intraformational Barriers, CRC-2b Injection Zone, Paaratte Formation, CO2CRC Otway Project, Otway Basin, Victoria. CO2CRC Report No. **RPT12-3532**, 84 pp.

Darling, T., 2005. Well Logging and Formation Evaluation. Elsevier Inc., Oxford, UK. 326 pp.

Dutton, S.P., Willis, B.J., White, C.D. and Bhattacharya, J.P., 2000. Outcrop characterization of reservoir quality and interwell scale cement distribution in a tide-influenced delta, Frontier Formation, Wyoming, USA. Clay Minerals, **35**, pp. 95–105.

Dutton, S.P., White, C.D., Willis, B.J. and Novakovic, D., 2002. Calcite cement distribution and its effect on fluid flow in a deltaic sandstone, Frontier Formation, Wyoming. AAPG Bulletin, **86**, pp. 2007–2021.

Geological Survey of Victoria, 1995. The Stratigraphy, Structure, Geophysics and Hydrocarbon Potential of the Eastern Otway Basin. Geological Survey of Victoria Report **103**, 241 pp.

Holdgate, G.R., Wallace, M.W., Daniels, J., Gallagher, S.J., Keene, J.B., Smith, A.J., 2000. Controls on Seaspray Group Sonic Velocities in the Gippsland Basin – A Multi-disciplinary Approach to the Canyon Seismic Velocity Problem. APPEA Journal, **40**(1), pp. 295-313.

Lee, K., Gani, M.R., McMechan, G.A., Bhattacharya, J.P., Nyman, S.L. and Zeng, X., 2007. Three-dimensional facies architecture and three-dimensional calcite concretion distributions in a tide-influenced delta front, Wall Creek Member, Frontier Formation, Wyoming. AAPG Bulletin, **91**(2), pp. 191–214.

McLean, M.A. and Blackburn, G.J., 2013. A New Regional Velocity Model for the Gippsland Basin. VicGCS Report **9**, Department of Primary Industries, Melbourne, Victoria. 62 pp.

Ott, H. and Oedai, S., 2015. Wormhole formation and compact dissolution in single- and two-phase CO_2-brine injections. Geophysical Research Letters, **42**, pp. 2270-2276.

Partridge, A.D., 2001. Revised stratigraphy of the Sherbrook Group, Otway Basin. In: Hill, K.C. and Bernecker, T. (Eds), Eastern Australian Basins Symposium, a Refocussed Energy Perspective for the Future, Petroleum Exploration Society of Australia, Special Publication, 455-464.

Taner, M.T., Koehler, F. and Sheriff, R.E., 1979. Complex Seismic Trace Analysis. Geophysics, **44**, pp. 1041–1063.

Taylor, G.T. and Gawthorpe, R.L., 2003. Basin-scale dolomite cementation of shoreface sandstones in response to sea-level fall. GSA Bulletin; **115**(10), pp. 1218–1229.

White, C.D., Willis, B.J., Dutton, S.P., Bhattacharya, J.P. and Narayanan, K., 2004. Sedimentology, statistics, and flow behavior for a tide-influenced deltaic sandstone, Frontier Formation, Wyoming, United States, outcrop and modern analogs in reservoir modeling. In: Grammer, G.M., Harris, P.M., Eberli, G.P. (Eds), Integration of outcrop and modern analogs in reservoir modeling, AAPG Memoir **80**, AAPG, Tulsa OK, pp. 129 –152.